Coordination Compounds of 9,10-Dihydro-9-oxa-10-phosphaphenanthrene-10-Oxide (DOPO) Ligands: Extremely High Thermostability and Ligand Oxidation in the Solid State

Daniela Goedderz,[a,b] Timmy Schäfer,[c] Johannes Klitsch,[a] Lais Weber,[a] Bettina Weber,[d] Olaf Fuhr,[e] Gerd Buntkowsky,[c] Frank Schönberger,[a] and Manfred Döring*[a]

Abstract: Different metal phosphinates and phosphonates were obtained containing zinc, calcium and magnesium as cations by means of a salt metathesis reaction with sodium salts of DOPO and DOPO-OH. The synthesized complexes $[Zn(DOPO)_2]_n$, $[Zn(DOPO\text{-}OH)_2]_n$ and $[Ca(DOPO)_2(H_2O)]_n$ are featured a polymeric structure. The open-ring metal phosphinate coordination compound $[Zn(DOPO)_2]_n$ is able to undergo a non-reversible thermally induced oxidative cyclisation to the corresponding metal phosphonate $[Zn(DOPO\text{-}OH)_2]_n$. The magnesium and calcium phosphinates cannot be oxidized to their corresponding metal phosphonate complexes. All organophosphorus compounds were analyzed by means of X-ray crystallography, NMR, TGA and TDMS. The oxidative cyclisation reaction of $[Zn(DOPO)_2]_n$ was investigated by DSC. Additionally, the coordination polymer $[Zn(DOPO)_2]_n$ can be transformed into a molecular complex by adding nitrogen ligands such as N-methylimidazole, whereby the phosphonate ligand changes from a bridging to a monodentate ligand. The synthesized coordination compounds exhibit very high thermostabilities of up to 520 °C.

Introduction

The applications of hybrid organic-inorganic materials like metal-organic frameworks (MOF) or coordination polymers are very numerous; they can be used for catalysis,[1] functional materials[2] and flame retardants.[3] Metal phosphinate chemistry enables an exceeding range of structural diversity and facilitates a vast range of applications.[3d,4] Metal phosphonates can possess a polymeric structure in which the metal ions are bridged by the coordinated ligands resulting in the formation of coordination polymers.[5] Such polymers exhibit metal cations in their backbone, which result in different properties compared to organic polymers.[6] Block et al. investigated bivalent metal-ion coordination polymers containing bridging phosphinate units throughout the 1960s.[7] Block identified a polymeric structure for some selected zinc phosphinates.[5,7d,8] Different poly(metal)phosphinates were patented as flame retardants for polyamides and polyesters in 1979.[9] In 2009 metal phosphinates as flame retardants, such as $Al[O_2P(C_2H_5)_2]_3$ (DEPAL) or $Zn[O_2P(C_2H_5)_2]_2$ (DEPZn), were established successfully in the flame retardant market.[10] Alkaline metal and alkaline earth metal salts of diorganylphosphinic acids are known for their flame retardant formulations in polyester and polyamides.[4c] Demadis et al.[11] reported the synthesis of different metal phosphonate salts containing PABPA, EDPA, TDTMP and EDPA as ligands with magnesium, calcium strontium and nickel as metal ions where the affinity of the metal ions for water is higher than for the phosphonate containing ligands. A coordination polymer was obtained for Ni-bpy-EDPA, in which the affinity of the metal ion for 4,4'-bpy as ligand is higher than the affinity for the phosphonate ligand. Vinas et al. reported new coordination polymers and complexes containing carboranylphosphinate ligands and different divalent metal ions.[6a,12] 9,10-dihydro-9-oxa-10-phosphaphenanthrene-10-oxide (DOPO) is used as a building block in flame retardants and can be synthesized through a condensation reaction from orthophenylphenol (OPP) and PCl_3 with zinc(II) chloride as catalyst with subsequent hydrolysis. DOPO as a monofunctional and reactive phosphororganic molecule and its derivatives as flame retardants show flame retardant efficiency in the gas and condensed phase.[13] The first aluminum phosphinate containing DOPO as ligand was synthesized in 1988 as a nucleating agent for polypropylene.[14] In 2001 metal phosphinates were invented as

flame retardants based on DOPO or DOPO-OH as organic ligands.[15] In 2006 different metal phosphinates premised on DOPO for epoxy resins, polyamides and polyesters were developed.[3d] After that different flame retardant formulations in PA 6.6 containing polymeric coordination compounds of DOPO were patented in 2014.[16] In this work synthesized coordination compounds containing zinc, magnesium and calcium as metal centers and DOPO or DOPO-OH as organic ligands were analyzed by single-crystal X-ray diffraction, NMR, DSC and TGA for the purpose of gaining an understanding of their thermal and thermo-oxidative behavior depending on the metal cation.

Results and Discussion

The metal phosphinates were synthesized by means of salt metathesis of suitable inorganic metal salts and sodium salts of DOPO, respectively DOPO-OH (Scheme 1) to form metal phosphinate and metal phosphonate complexes. The sodium salts of DOPO and DOPO-OH were obtained by adding an equimolar amount of sodium hydroxide solution in water. After the addition of 0 5 equivalent of the salts, the coordination compounds precipitate as white solid immediately. The solid structures of the coordination compounds $[Zn(DOPO)_2]_n$ and $[Zn(DOPO-OH)_2]_n$ (Scheme 1) were investigated by means of X-ray structure analysis and can be described as a phosphinate/phosphonate bridged one-dimensional-polymeric structure. The zinc phosphonate complex can be obtained through salt metathesis of DOPO-OH and the corresponding inorganic zinc salt or via solid-state oxidation starting from the zinc phosphinate complex. During this thermally induced oxidative cyclisation process in a closed construction, the release of water can be observed by using a tetrachlorocobaltate complex which reacts with water to form hexaaquacobaltate, turning from blue to pink. The process of solid-state oxidation from $[Zn(DOPO)_2]_n$ to $[Zn(DOPO-OH)_2]_n$ is a more atomically economical and efficient method, as the oxidation of DOPO to DOPO-OH using hydrogen peroxide. This thermally induced oxidation cannot be performed in the case of the magnesium or calcium complex.
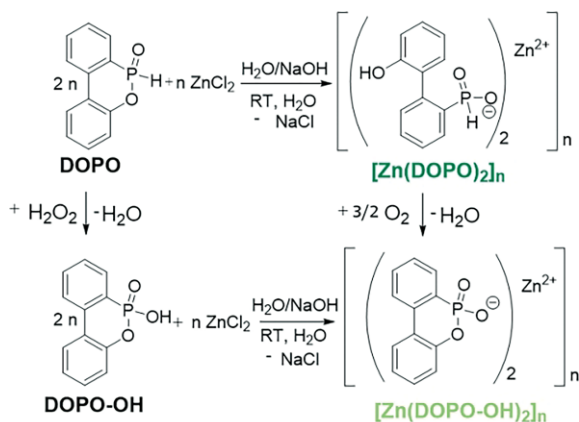
Scheme 1. Synthesis route to $[Zn(DOPO)_2]_n$ and $[Zn(DOPO-OH)_2]_n$.

A molecular complex, $[Zn(DOPO)_2(NMI)_2]$ was synthesized by suspending $[Zn(DOPO)_2]_n$ in methanol and adding N-methylimidazole (path A in Scheme 2).[17] The resulting compound shows a non-polymeric structure by coordinating the nitrogen containing base like N-methylimidazole, which is a strong Lewis base, and the phosphonate ligand with a changed coordination mode from bridged to monodentate. The synthesis of the resulting complex was performed in a one-pot reaction (path B in Scheme 2) starting from DOPO, N-methylimidazole and zinc nitrate hexahydrate in methanol or in two steps via $[Zn(DOPO)_2]_n$ as intermediate (path A in Scheme 2).
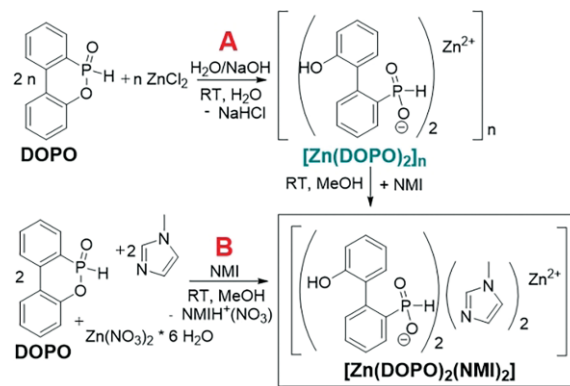
Scheme 2. Synthesis route to $[Zn(DOPO)_2(NMI)_2]$.

By using calcium chloride dihydrate it was possible to synthesize the polymeric coordination compound $[Ca(DOPO)_2(H_2O)]_n$ in which one equivalent of water could not be removed during the drying process (Scheme 3). This can be observed in the ^1H NMR spectra of the complex. Single crystals of the complex were obtained, and the coordinated water molecule can be monitored per repeating unit in the crystal structure (Figure 8). Crystals of $[Ca(DOPO-OH)_2]$ could not be obtained, but due to its thermal behavior (Figure 14) it is assumed that the crystal structure is similar to $[Mg(DOPO-OH)_2(H_2O)_6]$.
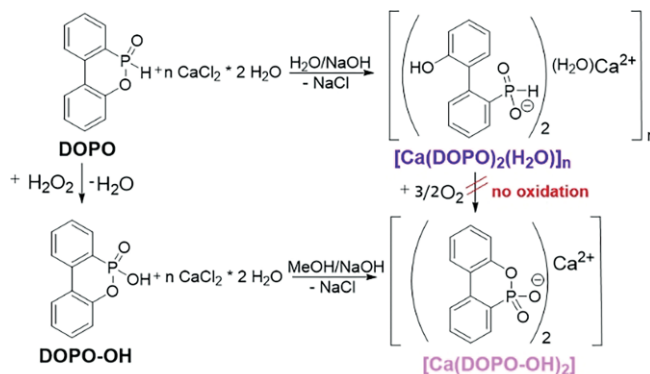
Scheme 3. Synthesis route to $[Ca(DOPO)_2(H_2O)]$ and $[Ca(DOPO-OH)_2]$.

Following the previous procedures for zinc-containing complexes, similar magnesium-containing salts were synthesized. Similar to $[Ca(DOPO)_2(H_2O)]_n$ no oxidative cyclization step can be executed to obtain the corresponding phosphonate coordination compound. The phosphonate complex $[Mg(DOPO-OH)_2(H_2O)_6]$ (Scheme 4) shows no polymeric structure, but its extremely high thermostability is similar to that of the corresponding phosphonate coordination compounds of calcium and zinc. Crystals of $[Mg(DOPO)_2]$ could not be obtained. Due

to the similar thermal behavior (Figure 14) with [Ca(DOPO)$_2$(H$_2$O)]$_n$ the crystal structure of the calcium- and magnesium-containing DOPO complexes is assumed to be similar.
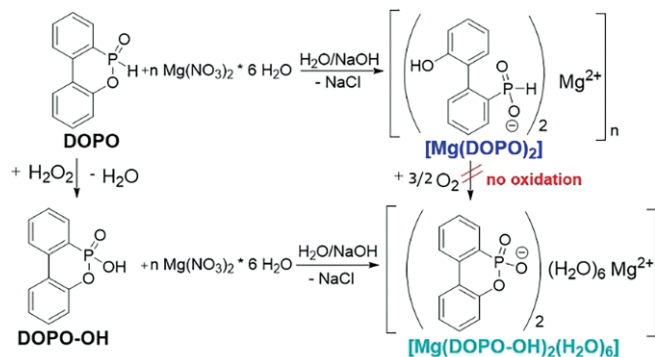
Scheme 4. Synthesis route to [Mg(DOPO)$_2$] and [Mg(DOPO-OH)$_2$(H$_2$O)$_6$].

Crystal Structures of DOPO- and DOPO-OH- Coordination Compounds and Salts

The solid structure of the metal phosphinate [Zn(DOPO)$_2$]$_n$ exhibits very high symmetry consisting of a one-dimensional polymeric chain with O–P–O-bridges (Figure 1). Two phosphinate groups and zinc atoms arranged in between form an eight-membered ring structure, whereas all zinc atoms are positioned in a line. These rings are linked together by the zinc atoms creating the main polymer chain structure. The crystal system is orthorhombic with the space group Iba2. Due to the hydrogen bond bridges between the phenolic group and the phosphinate group free rotation around the single bonds is restricted, resulting in a stiff configuration of the DOPO ligands. Thus, all DOPO ligands are aligned consistent leading to a one dimensional polymeric chain with O–P–O-bridges. The elementary cell consists of one zinc atom and one DOPO moiety, which has a coordinative covalent bond between the oxygen atom O1 and the metal cation. An enhanced opening of the solid structure shows the zinc atoms of the four repeating units being arranged on a horizontal line, whereas the distance between the metal centers amounts to 4.11 Å.

Two DOPO groups are arranged opposite each other forming an eight-membered ring with two zinc atoms coordinating the oxygen atoms of the phosphinate groups. The aromatic rings

of the phosphaphenanthrene groups located opposite each other in the eight membered ring form an angle of 29.64°, respectively. The two twisted aromatic rings of all phosphaphenanthrene ligands are aligned at angles of 89.04° and 90.96° to each other within the phosphaphenanthrene group (Figure 2). π-stacking occurs between similar 6+6π-phosphaphenanthrene ring planes in the polymeric structure. The distances between the parallel planes of the aromatic rings of the phosphaphenanthrene groups are 5.14 Å and 5.82 Å. Parallel aromatic rings are labeled in the same color in Figure 2 for [Zn(DOPO)$_2$]$_n$. The distances between C-atoms located in a similar position in the aromatic ring between parallel DOPO groups along the main chain are 8.13 Å (C5–C5) and 9 23 Å for C5 and C10 of the phosphaphenanthrene groups located on the opposite end of the main chain. Table 1 summarizes selected bond lengths and angles for [Zn(DOPO)$_2$]$_n$. The bond angles of O1-Zn1–O1 (127.97°), O2–Zn1–O1 (110.59° and 110.59°), O1-Zn1–O2 (97.66° and 97.66°) and O2–Zn1–O2 (112.88°) differ from the standard tetrahedron angle (109.5°), which means that [Zn(DOPO)$_2$]$_n$ is distorted slightly. Every zinc atom is a bridging atom which coordinates four ligands (two times about O1 and two times about O2) with the neighbored zinc atoms in the molecule. By considering a cross-section through the whole molecule it can be observed that the macromolecule is nonpolar on the far side of the center and strongly polar facing the center. The diffusion of water molecules or molecular oxygen in the cavities between the bulky ligands allows oxidative ring closure after drying in vacuo or under nitrogen atmosphere to take place, resulting in [Zn(DOPO-OH)$_2$]$_n$. The distance between the oxygen atom and the phosphorus atom in the phosphaphenanthrene group is
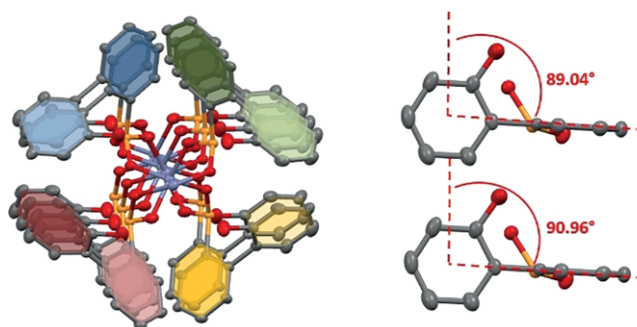
Figure 2. Front view of the crystal structure of [Zn(DOPO)$_2$]$_n$ with highlighted planes of the aromatic rings in all parallel DOPO groups. Every color points out parallel aromatic rings. Hydrogen atoms have been omitted for clarity.
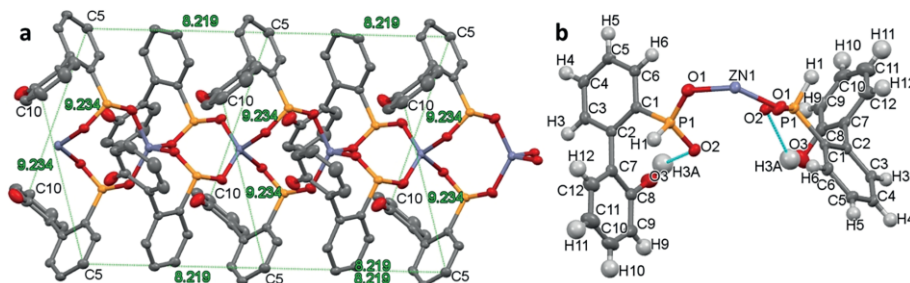
Figure 1. Crystal structure of [Zn(DOPO)$_2$]$_n$ (a: side view, b: elemental cell). Hydrogen atoms have been omitted for clarity. Hydrogen bonds are illustrated by blue dotted lines in [Zn(DOPO)$_2$]$_n$ (b).

Table 1. Bond angles and distances for the coordination compounds and salts.

Compound	[Zn(DOPO)$_2$]$_n$	[Zn(DOPO-OH)$_2$]$_n$	[Zn(DOPO)$_2$(NMI)$_2$]	[Ca(DOPO)$_2$(H$_2$O)]$_n$	[Mg(DOPO-OH)$_2$(H$_2$O)$_6$]
P1–O1/O2 [Å]	1.504/ 1.523	1.602/ 1.487	1.520/ 1.493[a]	1.514/ 1.490	1.608/ 1.498
M1–O1 [Å]	1.926	–	1.969[b]	2.338	1.995–2.214
M1–O2 [Å]	1.956	1.931	–	2.288	–
P1–C1 [Å]	1.794	1.782	1.801	1.803	1.776
O1–P1–O2 [°]	115.03	104.32	116.17	113.75	116.83
O1–M1–O1 [°]	127.97	–	–	–	_[d]
O1–M1–O4 [°]	–	–	109.88[c]	91.89	_[d]
O2–M1–O5 [°]	–	108.33	–	92.29	_[d]
O2–M1–O2 [°]	112.88	–	–	–	_[d]
O3–M1–O6 [°]	–	113.21	–	–	_[d]
Crystal system/ space group	O[d]/, I b a 2	M[e]/, P2$_1$/c	T[f]/, P - 1	M[e]/, P 2$_1$	M[e]/, C 2/c

[a] P2–O4: 1.519 Å; P2–O5: 1.494 Å; P3–O7: 1.506 Å; P3–O8: 1.493 Å; P4–O10: 1.517 Å; P4–O11: 1.492 Å. [b] Zn1–O4: 1.929 Å; Zn2–O7: 1.936 Å; Zn2–O10: 1.970 Å. [c] O7–Zn2–O10: 108.67°. [d] O6–Mg1–O6: 90.15°; O6–Mg1–O5: 86.43°; O5–Mg1–O4A: 79.26°; O5–Mg1–O4B: 96.93°; O4A–Mg1–O4B: 93.64°; O4B–Mg1–O4A: 93.64°; O4A–Mg1–O4A: 79.25°; O4B–Mg1–O5: 96.93°; O4A–Mg1–O5: 79.26°; O5–Mg1–O6: 86.43°; O4B–Mg1–O5: 82.74°; O6–Mg1–O5: 94.00°; O4B–Mg1–O4A: 25.26°; O4A–Mg1–O4B: 25.26°. [e] Orthorhombic. [f] Monoclinic. [g] Triclinic.
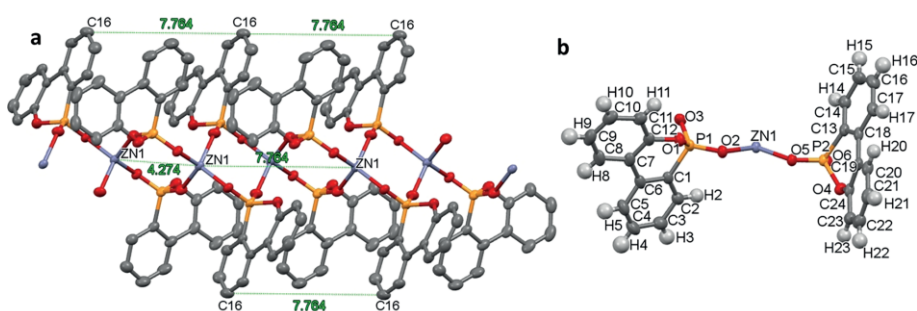
Figure 3. Crystal structure of [Zn(DOPO-OH)$_2$]$_n$ (a: side view, a: elemental cell). Hydrogen atoms have been omitted for clarity.

significantly shorter in [Zn(DOPO)$_2$]$_n$ (3.94 Å) than in the corresponding [Ca(DOPO)$_2$(H$_2$O)]$_n$ (4.08 Å and 4.09 Å) complex. The angles of the aromatic rings in the phosphaphenanthrene groups (measured on the side where the phosphorus and oxygen atom are located in the phosphaphenanthrene group) are smaller for the zinc complex (89.04° and 90.96°) than for the calcium complex (93.55° and 97.59°). The steric (or dimensional) proximity in the zinc complex promotes oxidative cyclization in the solid state, whereas the larger distance in the calcium complex may hinder a ring-closing oxidation mechanism.

The arrangement of the atoms in the ligands of [Zn(DOPO-OH)$_2$]$_n$ is not determined by intramolecular interactions such as hydrogen bond bridges. Figure 3 shows the elemental cell and the side view of the polymeric structure. The crystal system is monoclinic with space group P2$_1$/c. The front view (Figure 4b) shows that the coordination centers are not oriented in a line. The bond angles of O5–Zn1–O2 (108.33°), O2–Zn1–O6 (102.74°), O6–Zn1–O3 (113.21°), O5–Zn1–O3 (105.42°), O3–Zn1–O2 (116.06°) and O5–Zn1–O6 (111.11°) are closer to the standard tetrahedron angle than in the complex [Zn(DOPO)$_2$]$_n$ showing smaller distortion. Table 1 summarizes the bond length of [Zn(DOPO-OH)$_2$]$_n$. As in the complex [Zn(DOPO)$_2$]$_n$, every zinc atom coordinates four ligands, and the polymer is polar facing the center and non-polar on the far side of the center (cross section in Figure 4b). The distances between the metal centers in the molecule are 4.27 and 4.11 Å. When examining the side
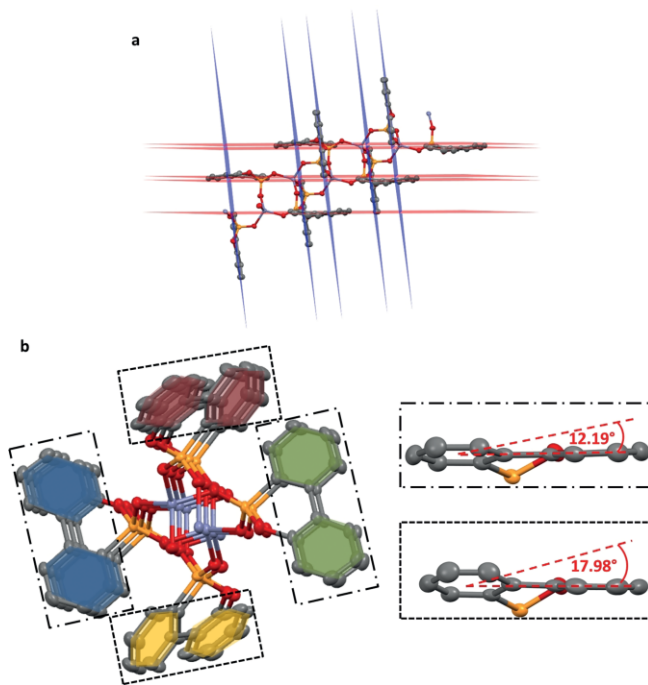
Figure 4. Side view of [Zn(DOPO-OH)$_2$]$_n$ with orthogonal DOPO-OH groups (a). Front view of the crystal structure of [Zn(DOPO-OH)$_2$]$_n$ with highlighted planes of the aromatic rings in all parallel DOPO groups (b). Every color points out parallel aromatic rings. Hydrogen atoms have been omitted for clarity.

view (Figure 3), the double-row arrangement of the central atoms and the tightened packing of the ligands in the polar center attracts attention.

The crystal structure of $[Zn(DOPO-OH)_2]_n$ shows a non-parallel arrangement of each aromatic ring in the phosphaphenanthrene group. All ligands strive to take the maximum distance to each other, leading to an orientation in which the coordination centers are not arranged on a line. The planes of the DOPO-OH groups located on the opposite of the main chain are oriented at an angle of 83.08° to each other. This results in different angles of the twisted aromatic rings in a DOPO-OH group.

The DOPO-OH groups with a neighboring DOPO-OH group near the surface of the aromatic ring plane show twisted aromatic rings with angles of 17.98° to each other (red planes in Figure 4 a). The other DOPO-OH groups show twisted aromatic rings with smaller angles of 12.19° to each other (Figure 4b). The bond angle of O1–P1–O2 is decreased in $[Zn(DOPO-OH)_2]_n$ to 104.32°. as compared to $[Zn(DOPO)_2]_n$ with 115.03° (Table 1). In the unit cell, the bond angles of O–M–O which connects the two DOPO/DOPO-OH groups is larger in $[Zn(DOPO)_2]_n$ (O1-Zn1–O1: 127.97°) than in $[Zn(DOPO-OH)_2]_n$ (O2–Zn1–O5: 108.33°). The ligands in $[Zn(DOPO-OH)_2]_n$ are positioned at a greater distance to each other, whereas the DOPO groups in $[Zn(DOPO)_2]_n$ have a stiff configuration due to the hydrogen bonds.

The crystal structure of $[Zn(DOPO)_2(NMI)_2]$ is triclinic with space group $P\bar{1}$. All asymmetric units of the crystals contain twinning crystals with two zinc ions, four DOPO ligands and four N-methylimidazole ligands. The bond angles between the zinc atoms and the coordinated ligands are different in the twinning crystals containing Zn1 and Zn2. The twinning crystal comprising Zn1 (Figure 5b) shows the following bond angles: N1–Zn1–O4: 98.60°; O4–Zn1–O1: 109.88°; O1-Zn1–N1: 107.93°; N1–Zn1–N3: 119.08°; N3–Zn1–O1: 104.35° and N3–Zn1–O4: 116.74°. The bond angles containing Zn2 are not the same, but the difference from those containing Zn1 is not significant (N5–Zn2–N7: 117.97°; N7–Zn2–O7: 99.31°; O7–Zn2–O10: 108.67°; O10–Zn2–N5: 103.87°; N5–Zn2–O7: 118.27° and O10–Zn2–N7: 108.42°).

The structure of $[Zn(DOPO)_2(NMI)_2]$ is molecular, but the angles of the twisted aromatic rings of the DOPO group, in the unit cell are all different, but are similar to $[Zn(DOPO)_2]_n$ (86.27°, 88.27°, 87.90° and 89.13° in Figure 6a. The DOPO groups in the twinning crystals which are coordinated to the same zinc atom are not parallel. The planes have angles of 16.53° and 12 21° between the aromatic rings connected to the phosphinate group and 6.95° and 4.31° for the phenol groups (Figure 6b). The distance between the two zinc atoms in the twinning crystal is 14.26 Å. The heterocyclic ligands N-methylimidazole are located in angles of 79.03° (Zn2 moiety) and 76.93° (Zn1 moiety) to each other.

Subsequent oxidation from the phosphinate to the phosphonate complex is also not possible, as $[Mg(DOPO)_2]$. $[Mg(DOPO-OH)_2(H_2O)_6]$ has an orthorhombic crystal system with the space group C 2/c. In contrast to the corresponding zinc compound, no polymeric structure was obtained, but the
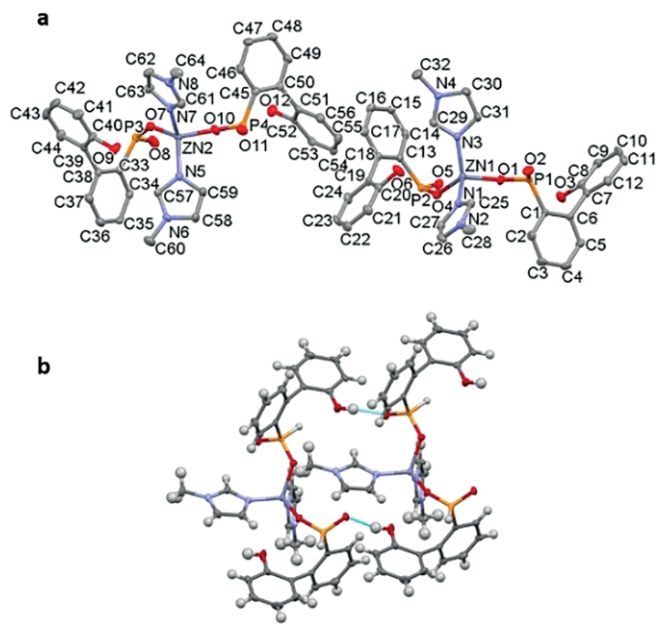
Figure 5. Crystal structure of $[Zn(DOPO)_2(NMI)_2]$ (a). Hydrogen atoms have been omitted for clarity. Hydrogen bonds are illustrated by dotted blue lines in $[Zn(DOPO)_2(NMI)_2]$ (b).
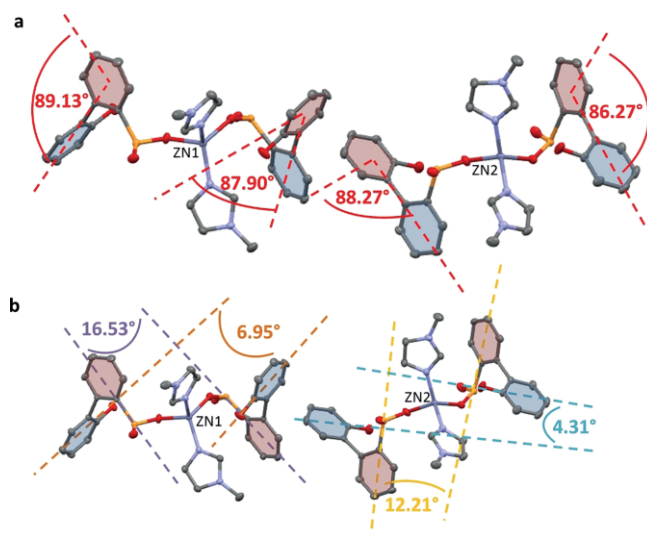
Figure 6. Crystal structure of $[Zn(DOPO)_2(NMI)_2]$ with highlighted planes of the aromatic rings in the DOPO groups (a) and to each other (b). Hydrogen atoms have been omitted for clarity.

thermostability of this complex is similar to the phosphonate complexes of calcium and zinc.

The unit cell consists of one hexaaquamagnesium cation and two symmetrical equivalent phosphonate anions with two water molecules, which show a strong interaction in the form of hydrogen bond linkage (blue dotted line in Figure 7a). The affinity of the Mg^{2+} is higher for water than for DOPO-OH as ligand. The aromatic rings of the phosphaphenanthrene group are twisted by 18.96° (Figure 7b). The distance of the magnesium atom and O4B is significantly higher than the distance between the metal and the other oxygen atoms. The bond an-

Figure 7. Crystal structure of [Mg(DOPO-OH)$_2$(H$_2$O)$_6$] with hydrogen bridge bond situation (a) and angle of the aromatic rings in the DOPO-OH group (b).

Figure 8. Crystal structure of [Ca(DOPO)$_2$(H$_2$O)]$_n$ (a). Side view of [Ca(DOPO)$_2$(H$_2$O)]$_n$ (b). Hydrogen atoms have been omitted for clarity.

gle of O1–P1–O2 is similar to that of the zinc complexes with 116.83°.

[Ca(DOPO)$_2$(H$_2$O)]$_n$ has an orthorhombic crystal system with the space group P 2$_1$. It shows a polymeric structure similar to [Zn(DOPO)$_2$]$_n$ and [Zn(DOPO-OH)$_2$]$_n$, but oxidative cyclisation to the corresponding phosphonate complex is not possible.

The crystal structure is shown in Figure 8, and important bond angles and length are presented in Table 1. Hydrogen bond bridges are not formed in the solid structure. Calcium has an octahedral arrangement of ligands, and the O–Ca–O bond angles differ slightly from the ideal octahedral angle of 90° (O1–Ca1–O5: 80.50°; O1–Ca1–O7: 83.11°; O1–Ca1–O7: 110.68°; O1–Ca1–O4: 91.89°; O2–Ca1–O7: 80.72°; O2–Ca1–O5: 92.29°; O2–Ca1–O7: 83.50°; O2–Ca1–O4: 94.56°; O4–Ca1–O7: 102.52°; O7–Ca1–O5: 81.97°; O5–Ca1–O7: 85.56°; O7–Ca1–O4: 91.84°). As already established in the literature, the distance between oxygen and metal atoms increases with increasing coordination number.[18] All zinc complexes have O1/2-M1 distances ranging between 1.93 and 1.97 Å, whereas the distance between O1/2-M1 is increased in [Mg(DOPO-OH)$_2$(H$_2$O)$_6$] and [Ca(DOPO)$_2$(H$_2$O)]$_n$ up to 2.34 Å.

Similar to [Zn(DOPO-O)$_2$]$_n$ the metal atoms are not oriented in a line, but they are closer with smaller cavities. The distance between two bridged calcium atoms is 3.97 Å, whereas two calcium atoms oriented in line are separated by a distance of 7.81 Å (Figure 8). One water molecule is coordinated with equal distances from the oxygen and the metal atom per repeating unit.

The distance between two parallel phosphaphenanthrene groups is 7.81 Å. The aromatic rings in the phosphaphenanthrene groups are twisted, with an angle of 86.45° or 82.41° (Figure 9).

Figure 9. Front view of the crystal structure of [Ca(DOPO)$_2$(H$_2$O)]$_n$ with highlighted planes of the aromatic rings (a) in all parallel DOPO groups (b). Every color points out parallel aromatic rings. Hydrogen atoms are omitted for clarity.

NMR Characterization in the Liquid and Solid Phases

The influence of the metal atom on the chemical shift in the liquid phase for ^{31}P NMR is shown in Figure 10 and Table 2, in which all ^{31}P NMR shifts of the phosphinate and phosphonate complexes are summarized. The chemical shift of the phosphorus atom is dependent on the oxygen content in the chemical environment and the metal of the complex. The ^{31}P NMR spectra show an upfield shift in the following order: Zn < Mg < Ca and DOPO < DOPO-OH.

[Ca(DOPO)$_2$(H$_2$O)]$_n$ and [Mg(DOPO-OH)$_2$(H$_2$O)$_6$] have coordinated water molecules effecting very broad ^{31}P NMR signals in the liquid phase. The two ^{31}P NMR signals for [Ca(DOPO-OH)$_2$] can result from coordinated water as in [Ca(DOPO)$_2$(H$_2$O)]$_n$ or from structural disorders, which can also effect the very broad

Figure 10. ^{31}P NMR spectra of all phosphinate and phosphonate complexes in the liquid phase with [D_6]DMSO as solvent. H_3PO_4 was used as standard.

Table 2. ^{31}P NMR shifts of all coordination compounds and salts in the liquid phase with [D_6]DMSO as solvent. (s = singlet, bs = broad signal).

Compound	^{31}P NMR chemical shift in ppm (121.60 MHz/ 298 K/[D_6]DMSO)
[Zn(DOPO)$_2$]$_n$	17.13 (s)
[Zn(DOPO-OH)$_2$]$_n$	3.51 (s)
[Zn(DOPO)$_2$(NMI)$_2$]	16.63 (s)
[Ca(DOPO)$_2$(H$_2$O)]$_n$	6.32 (bs)
[Ca(DOPO-OH)$_2$]	−0.37: −1.75 (bs)
[Mg(DOPO)$_2$]	9.84 (s)
[Mg(DOPO-OH)$_2$(H$_2$O)$_6$]	−1.84 (bs)

^{31}P CP MAS signal. The influence of the metal ion on the ^{31}P chemical shift is known in the literature.[19]

The cationic potential (charge/radius) of the counterions affects the ^{31}P NMR chemical shift by an increased ^{31}P NMR chemical shift with an increasing cationic potential (Figure 11). This trend can be observed in both metal complexes with
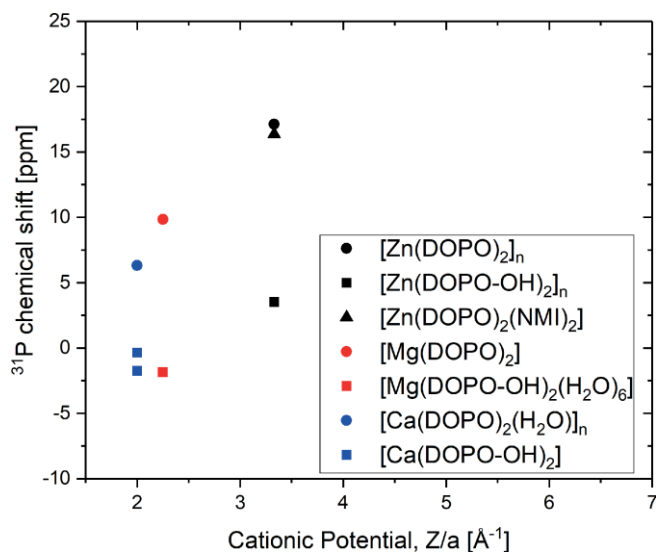
Figure 11. Correlation between ^{31}P NMR chemical shift in the liquid phase and the counterion potential (charge/radius) for all complexes.

DOPO or DOPO-OH as ligands, whereas the level of the linear trend is shifted to smaller ^{31}P NMR chemical shifts for the DOPO-OH-containing complexes. Similar correlations between the cationic potential and the ^{31}P chemical shift were reported by Brow et al. for metaphosphate glasses.[20] The ionic radii were taken from Shannon et al.[21] The correlation of the counterion as well as the ligand on the ^{31}P chemical shift is shown in Figure 11.

The ^{31}P CP MAS spectra in the solid state of the DOPO containing complexes (Figure 12 and Table 3) show an increased splitting of the signal in the following order: Ca < Mg < Zn. A coordination of DOPO-OH leads to a broad ^{31}P CP MAS signal. The difference becomes obvious when comparing [Zn(DOPO-OH)$_2$]n and [Mg(DOPO-OH)$_2$(H$_2$O)$_6$]. The ligand DOPO-OH is coordinated in [Zn(DOPO-OH)$_2$]$_n$ to the zinc ion, whereas only water is coordinated to the magnesium ion in [Mg(DOPO-OH)$_2$(H$_2$O)$_6$]$_n$.
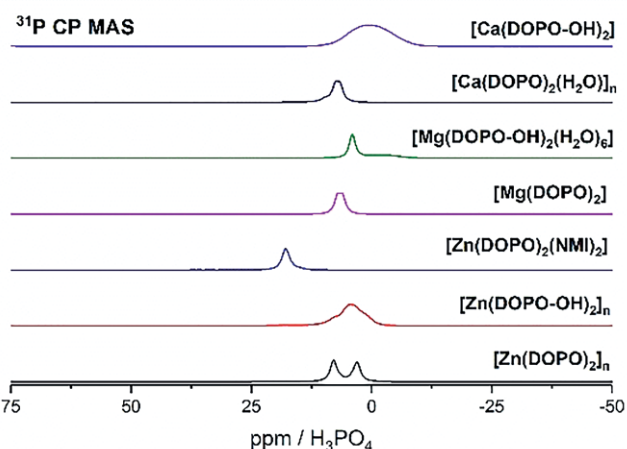
Figure 12. ^{31}P CP MAS spectra of the metal salts of DOPO and DOPO-OH, measured at 10 kHz spinning at room temperature.

Table 3. ^{31}P CP MAS shifts of all coordination compounds and salts.

Compound	^{31}P NMR chemical shift in ppm (10 kHz spinning at room temperature)		
[Zn(DOPO)$_2$]$_n$	9.7	7.4	6.8
[Zn(DOPO-OH)$_2$]$_n$	7.0	6.2	–
[Zn(DOPO)$_2$(NMI)$_2$]	8.0	3.1	–
[Ca(DOPO)$_2$(H$_2$O)]$_n$	7.4	6.8	–
[Ca(DOPO-OH)$_2$]	4.1	−2.6	–
[Mg(DOPO)$_2$]	7.5	4.3	1.0
[Mg(DOPO-OH)$_2$(H$_2$O)$_6$]	9.7	7.4	6.8

An influence of the cationic potential of the counterions on the ^{31}P CP MAS chemical shift (Figure 13) is also present in the solid state, but in reverse order. An increased ^{31}P CP MAS chemical shift goes along with a decreased cationic potential. This trend is more pronounced for the DOPO-containing complexes, whereas the DOPO-OH-containing complexes show no clear trend due to broad signals. The cationic potential decreases with increasing ^{31}P chemical shift in the following order: Ca > Mg > Zn.
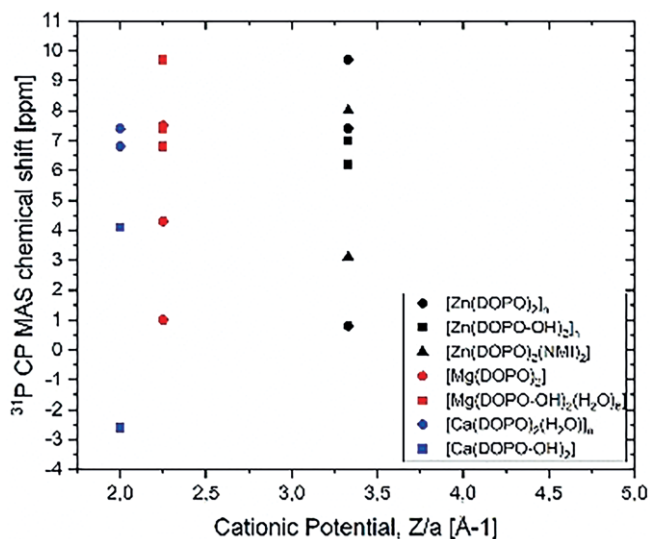
Figure 13. Correlation between ^{31}P chemical shift and the counterion potential (charge/radius) for all complexes in the solid state.

Figure 14. TGA of $[Zn(DOPO)_2]_n$, $[Zn(DOPO-OH)_2]_n$, $[Zn(DOPO)_2(NMI)_2]$, $[Mg(DOPO)_2]$, $[Mg(DOPO-OH)_2(H_2O)_6]$, $[Ca(DOPO)_2(H_2O)]_n$ and $[Ca(DOPO-OH)_2]$ in nitrogen atmosphere (10 K/min).

Thermal Properties of the Coordination Complexes and Salts

The TGA curves of all coordination compounds and salts in nitrogen atmosphere compounds are pictured in Figure 14 and listed in Table 4. To investigate the decomposition behavior in more detail, TDMS (vacuum) and ^{31}P CP MAS experiments with thermal treated samples under air atmosphere were performed.

Concerning the thermostability of $[Zn(DOPO)_2]_n$ the thermogravimetric investigation points to a concise step near 200 °C (Figure 15). To investigate this step more closely, a DSC analysis was performed, which indicates an exothermic reaction step of the coordination compound with a maximum at 213 °C (Figure 15), which is due to the oxidative cyclization to $[Zn(DOPO-OH)_2]_n$ under release of water. After the conversion of the phosphinate into the DOPO-based bridging complex is complete, the TGA-curve is similar to that of the highly thermostable

Table 4. Thermal properties of the coordination compounds and salts by thermal gravimetric analysis in nitrogen.

Compound	$T_{2\%}$ [°C]	$T_{5\%}$ [°C]	Residue at 700 °C [%]
$[Zn(DOPO)_2]_n$	206	388	62
$[Zn(DOPO-OH)_2]_n$	515	533	63
$[Zn(DOPO)_2(NMI)_2]$	152	176	40
$[Ca(DOPO)_2(H_2O)]$	157	177	35
$[Ca(DOPO-OH)_2]$	481	522	48
$[Mg(DOPO)_2]$	174	212	57
$[Mg(DOPO-OH)_2(H_2O)_6]$	370	574	66

$[Zn(DOPO-OH)_2]_n$ losing 5 wt.-% at 388 °C. This oxidation will also take place during extrusion of $[Zn(DOPO)_2]_n$ as a flame retardant in PA 6.6. Thus, after the extrusion process most of the phosphinate complex will be converted to $[Zn(DOPO-OH)_2]_n$ in
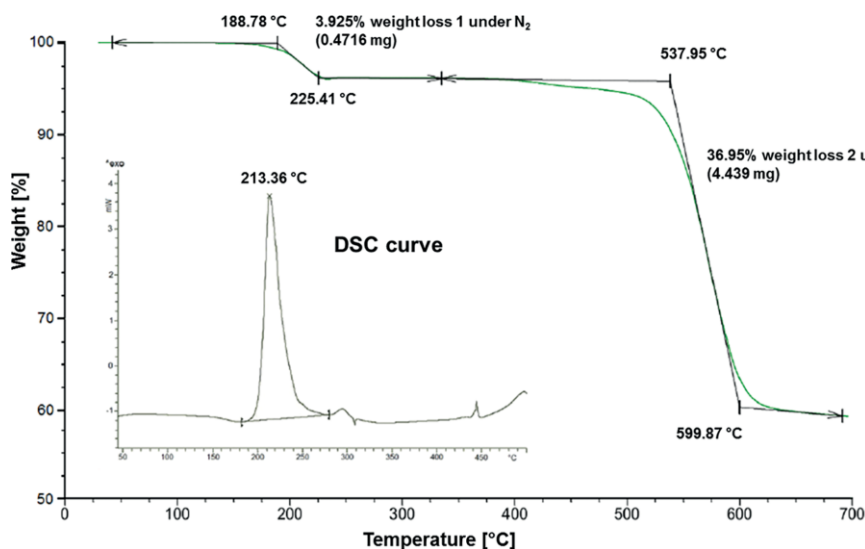
Figure 15. DSC and TGA curve of $[Zn(DOPO)_2]_n$ in nitrogen atmosphere with oxidative cyclization under water release (heating rate: 10 K/min).

the polymer matrix.[22] The oxidative cyclization step is not reversible.[3c]

The different thermal behavior of the thermal gravimetric analysis of the calcium complexes $[Ca(DOPO)_2(H_2O)]_n$ and $[Ca(DOPO-OH)_2]$ is pictured in Figure 15. The thermal behavior of $[Ca(DOPO-OH)_2]$ is very similar to that of $[Mg(DOPO-OH)_2(H_2O)_6]$, which has no polymeric structure.

The comparison of the TGA under air and nitrogen reveals no significant difference in thermal behavior with respect to the residue at 700 °C (Figure 14 and Figure 16). Decomposition under air progresses faster, especially for $[Mg(DOPO)_2]$, $[Ca(DOPO)_2(H_2O)]_n$ and $[Zn(DOPO)_2]_n$ (Table 5).
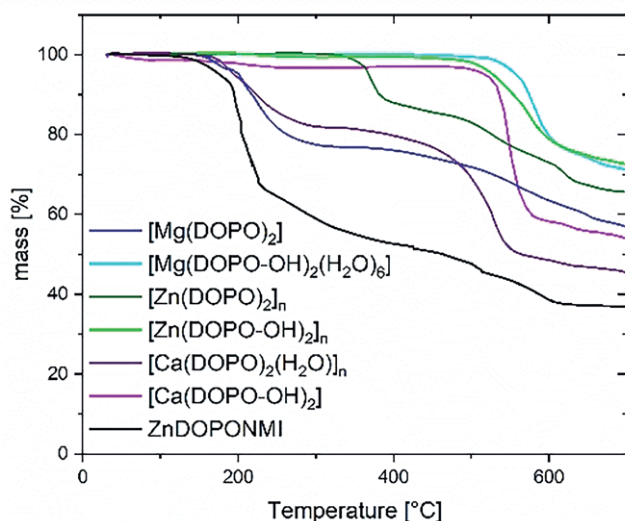
Figure 16. TGA of $[Zn(DOPO)_2]_n$, $[Zn(DOPO-OH)_2]_n$, $[Zn(DOPO)_2(NMI)_2]$, $[Mg(DOPO)_2]$, $[Mg(DOPO-OH)_2(H_2O)_6]$, $[Ca(DOPO)_2(H_2O)]_n$ and $[Ca(DOPO-OH)_2]$ in air atmosphere (10 K/min).

Table 5. Thermal properties of the coordination compounds and salts by thermal gravimetric analysis in air.

Compound	$T_{2\%}$ [°C]	$T_{5\%}$ [°C]	Residue at 700 °C [%]
$[Zn(DOPO)_2]_n$	355	364	66
$[Zn(DOPO-OH)_2]_n$	498	524	73
$[Zn(DOPO)_2(NMI)_2]$	136	176	37
$[Ca(DOPO)_2(H_2O)]_n$	176	193	45
$[Ca(DOPO-OH)_2]$	181	514	54
$[Mg(DOPO)_2]$	163	201	57
$[Mg(DOPO-OH)_2(H_2O)_6]$	532	557	71

The thermostability of $[Zn(DOPO)_2(NMI)_2]$ is significantly lower as compared to the corresponding polymeric complex $[Zn(DOPO)_2]_n$ due to the decomposition of the N-methylimidazole ligands (Figure 20). In addition, no oxidative cyclization step can be observed.

For $[Mg(DOPO)_2]$, similar to $[Ca(DOPO)_2(H_2O)]_n$, more than one decomposition step was observed. Decomposition starts at a temperature slightly lower than 200 °C. A residue of 57 % at 700 °C is obtained, which indicates the release of one phosphinate moiety. TDMS results show the release of phenyl derivatives (Figure 20).

The thermal properties of the calcium coordination compounds and salts are similar to those of the corresponding magnesium coordination compounds and salts. The TG analysis of $[Ca(DOPO-OH)_2]$ shows a very high thermal stability of about 500 °C. The decomposition of the DOPO-derivative structure starts at 150 °C due to the evaporating water in the macromolecule. The significantly higher thermostability of $[Ca(DOPO-OH)_2]$ indicates that there is no water molecule which can be evaporated while heating.

All coordination compounds and salts were thermally treated at 600 °C and ^{31}P CP MAS were measured in the solid state. The ^{31}P CP MAS spectra are pictured in Figure 17, and the results are listed in Table 6.
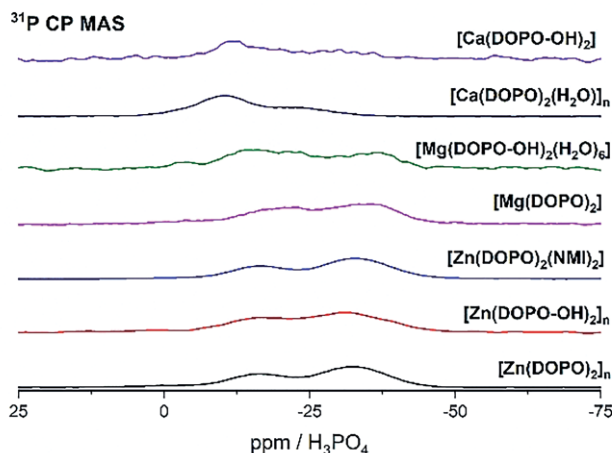
Figure 17. ^{31}P CP MAS spectra of the thermally treated samples.

Table 6. ^{31}P NMR shifts of all coordination compounds and salts after thermal treatment.

Compound	^{31}P CP MAS chemical shift in ppm (10 kHz at room temperature)	
$[Zn(DOPO)_2]_n$	−18.2	−33.6
$[Zn(DOPO-OH)_2]_n$	−17.8	−31.0
$[Zn(DOPO)_2(NMI)_2]$	−18.2	−32.4
$[Ca(DOPO)_2(H_2O)]$	−20.7	−34.8
$[Ca(DOPO-OH)_2]_n$	−15.8	−35.7
$[Mg(DOPO)_2]$	−10.5	−22.1
$[Mg(DOPO-OH)_2(H_2O)_6]$	−11.8	−29.2

Only broad signals are obtained which cannot be assigned to the corresponding phosphates as main decomposition products. The ^{31}P CP MAS spectra of $Zn_3(PO_4)_2$, $Ca_3(PO_4)_2$ and $Mg_3(PO_4)_2$ are shown in Figure 18, and the results are listed in Table 7. This is in accordance with the results obtained from TG analysis, because the residue at 700 °C exceeds the expected amount significantly, assuming phosphates as primary decomposition products. An illustrative ^{13}C CP MAS of thermally treated $[Zn(DOPO)_2(NMI)_2]$ in Figure 19 shows that thermal decomposition leads to different carbon-containing species which are chemically similar to DOPO or DOPO-OH derivatives (see ^{13}C CP MAS in supporting information). This means that no total conversion to a phosphate species took place at 700 °C and that some DOPO/DOPO-OH ligands remain in the residue.

TDMS results are shown in Figure 20 for the phosphinate complexes, whereas the results for the phosphonate complexes can be found in the supporting information. Whilst only the
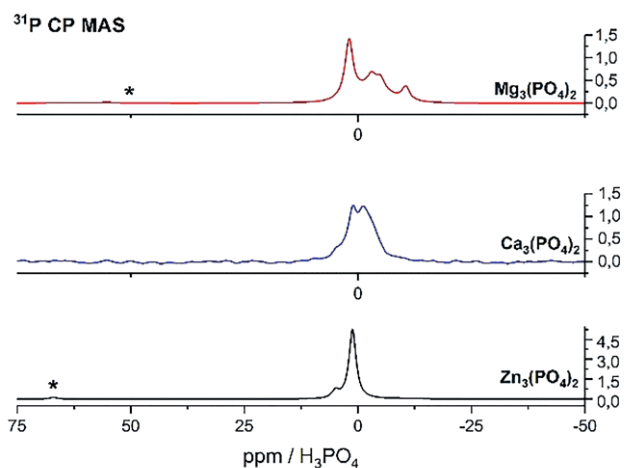
Figure 18. ³¹P CP MAS spectra of zinc phosphate, calcium phosphate, and magnesium phosphate. * spinning sideband.

Table 7. ³¹P NMR shifts of zinc phosphate, calcium phosphate, and magnesium phosphate.

Compound	^{31}P CP MAS chemical shift in ppm (10 kHz at room temperature)			
$Zn_3(PO_4)_2$	4.6	1.2	–	–
$Ca_3(PO_4)_2$	1.2	−1.2	–	–
$Mg_3(PO_4)_2$	1.9	−3.2	−4.7	−10.4

release of aromatic fragments can be observed for the DOPO-OH complexes, the evolution of DOPO fragments can be ob-
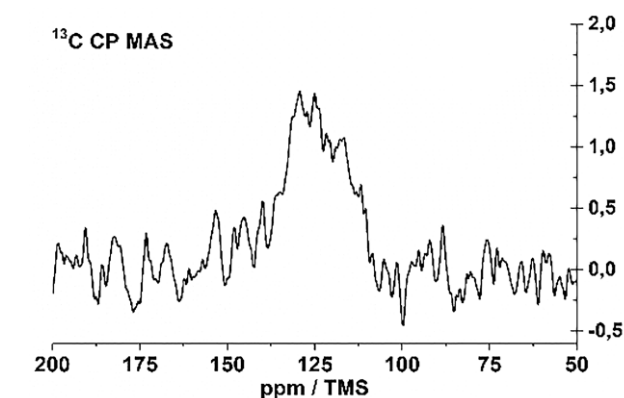
Figure 19. ¹³C NMR shifts of thermal treated [Zn(DOPO)₂(NMI)₂].

served for the DOPO-containing complexes. The TDMS results show an increased release of phosphorus-containing fragments in the gas phase with decreasing oxygen content in the chemical environment of the phosphorus atom. The TDMS results indicate that the DOPO/DOPO-OH-ligands decompose due to the release of phosphorus-containing or aromatic fragments. The TGA and ³¹P CP MAS/¹³C CP MAS experiments are in accordance with the TDMS results, but they point out that decomposition to the corresponding phosphates is not completed at 700 °C. The thermally treated complexes still contain DOPO/DOPO-OH derivatives at high temperatures.
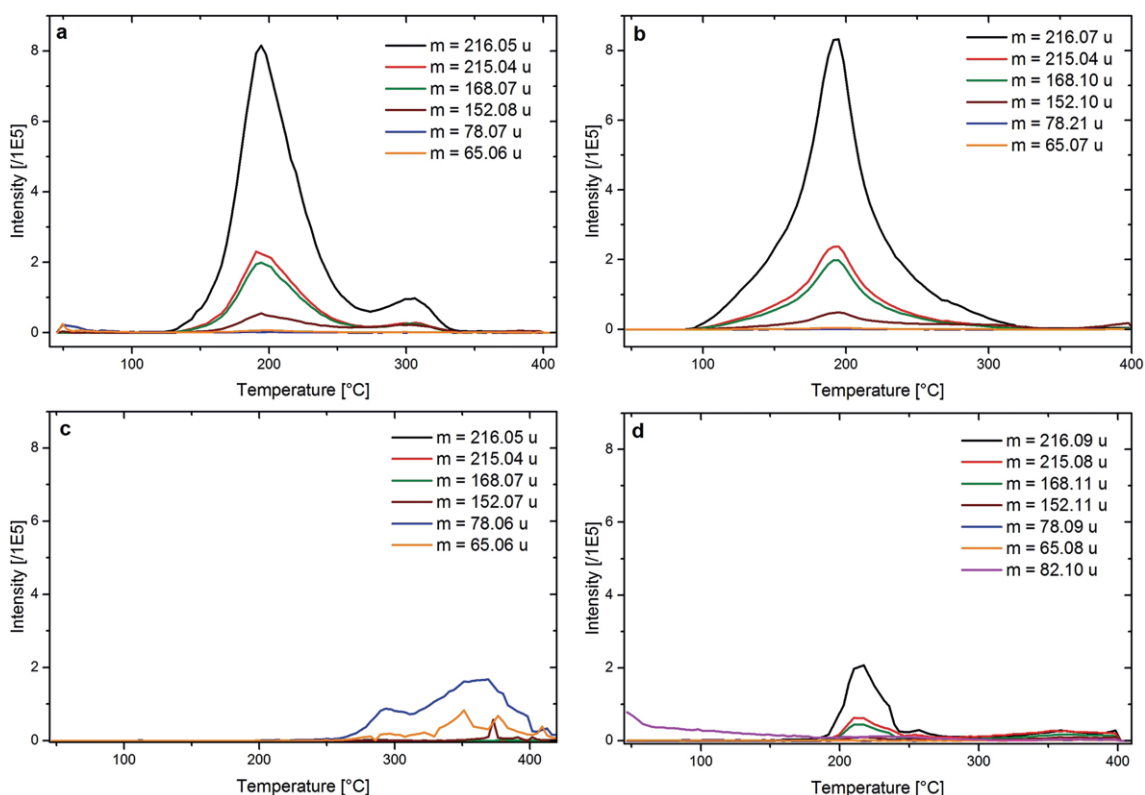
Figure 20. Thermodesorption mass spectra (TDMS) for [Ca(DOPO)₂(H₂O)]ₙ (top left), [Mg(DOPO)₂] (top right), [Zn(DOPO)₂]ₙ (bottom left) and [Zn(DOPO)₂(NMI)₂] (bottom right) in the temperature range of 40–400 °C **in vacuo**.

Conclusions

Different metal phosphinates and phosphonate coordination compounds and salts based on DOPO and DOPO-OH containing different metal atoms such as zinc, magnesium, and calcium were successfully synthesized. Where it was possible to obtain prepared crystals, the structures were analyzed by X-ray crystallography, which revealed that some of the coordination compounds exhibit polymeric structures. A thermal cyclization step of $[Zn(DOPO)_2]_n$ to the corresponding phosphonate $[Zn(DOPO\text{-}OH)_2]_n$ was investigated by DSC. This cyclization step is not possible for the corresponding calcium and magnesium coordination compounds. When the base N-Methylimidazole is added as neutral ligand, the polymeric structure of $[Zn(DOPO)_2]_n$ alters so that the phosphinate ligand changes from a bidentate to a monodentate ligand. This is possible due to the stronger Lewis character of the nitrogen-containing base compared to the phosphinate ligand. Certain complexes show very high thermostability with decomposition temperatures greater than 500 °C. Analysis of the residue after thermal decomposition showed that a certain amount of the DOPO/DOPO-OH-ligands remain at 700 °C, and that decomposition to the corresponding phosphates is not finished at this high temperature.

Experimental Section

Instrumentation and materials

The ^{1}H and ^{31}P NMR spectra of the metal complexes were measured in [D$_6$]DMSO with a spectrometer of Bruker type Ultrashield 300. Chemical shifts are reported as δ values relative to the solvent peak in ppm. Trimethylsilane was used as a standard. The thermogravimetric analyses were detected with a thermo balance of TA Instruments (type Q500) under nitrogen atmosphere and a heat release of 10 K/min.

All ^{31}P CP MAS measurements were performed on a Bruker Avance III HD 300 spectrometer (Rheinstetten, Germany) employing a 4 mm broadband H/X probe. Spectra were recorded at 7 T, corresponding to a frequency of 121.49 MHz for ^{31}P and 75.47 MHz for ^{13}C, at 10 kHz spinning, respectively, at room temperature. Spectra were referenced to phosphoric acid (0 ppm) for ^{31}P and adamantane for ^{13}C (+38.5 ppm) as external standards. The ramped CP-MAS sequence[23] was utilized with a contact time of 3.2 ms for ^{31}P and 3.0 ms for ^{13}C. The recycle delay was set to 2 s. and tppm decoupling[24] employing a 15° phase jump was applied during data acquisition. Approximately 60 mg of each sample was filled in a 4 mm ZrO$_2$ rotor.

The remaining residues after a thermal treatment of the substances at 700 °C were analyzed by using ssNMR experiments.

Single crystals were obtained by slow diffusion crystallization. A suitable crystal was selected and mounted on a Stoe IPDS2T diffractometer. The crystal was kept at 180.15 K during data collection. Using Olex2,[25] the structure was solved with the ShelXS[26] structure solution program using Direct Methods and refined with the ShelXL[27] refinement package using Least Squares minimization.

Deposition Number(s) 1989671 (for $[Zn(DOPO)_2]_n$), 1989672 (for $[Zn(DOPO\text{-}OH)_2]_n$), 1989673 (for $[Zn(DOPO)_2(NMI)_2]$), 1989674 (for $[Ca(DOPO)_2(H_2O)]_n$), and 1989675 (for $[Mg(DOPO\text{-}OH)_2(H_2O)_6]$) contain(s) the supplementary crystallographic data for this paper. These data are provided free of charge by the joint Cambridge Crystallo-graphic Data Centre and Fachinformationszentrum Karlsruhe Access Structures service www.ccdc.cam.ac.uk/structures.

Unless stated otherwise, solvents and chemicals were obtained from commercial sources and used without further purification. 9,10-dihydro-9-oxa-10-phosphaphenanthrene-10-oxide (DOPO) was purchased by Metadynea. 10-hydroxy-9,10-dihydro-9-oxa-10-phos-phaphenanthrene-10-oxide or 6-Hydroxydibenzo[c,e][1,2]oxaphos-phinin-6-oxide (DOPO-OH) was synthesized from DOPO accordingly, as previous reported.[28] DOPO and DOPO-OH were shredded in a mortar or a mill. Sodium hydroxide, zinc chloride, magnesium nitrate hexahydrate, zinc nitrate hexahydrate and methanol were purchased from commercial sources.

2.1 Synthesis of Poly(bis((2′-hydroxy-[1,1′-biphenyl]-2-yl)phosphi-nato)zinc(II))– $[Zn(DOPO)_2]_n$

In a 2-liter beaker, 108.09 g (500 mmol) of DOPO were suspended in 600 mL of water. In a second beaker 20.00 g (500 mmol) of sodium hydroxide were dissolved. After cooling the solution to room temperature, the sodium hydroxide solution was dropped to the DOPO-containing suspension while stirring. The beaker was rinsed with 100 mL of water and a clear solution was obtained. In a third beaker 73.37 g (250 mmol), zinc nitrate hexahydrate was dissolved in 250 mL of water. The resulting solution was added to the other solution rapidly while stirring. The beaker again was rinsed with 100 mL of water and a colorless solid appeared. The reaction mixture was stirred for 15 minutes. The product was filtered, washed with water and dried in vacuo (5 mbar, 130 °C).

Color: White. Yield: 121.8 g, 92 %. ^{1}H NMR (300.38 MHz, 298 K, [D$_6$]DMSO): δ = 9.74 (s, 2H); 7.68 (ddd, J = 12.4 Hz, 7.6 Hz, 1.4 Hz, 2H); 7.49 (tt, J = 7.6 Hz, 1.3 Hz, 2H); 7.31 (ddd, J = 7.7 Hz, 6.0 Hz, 1.4 Hz, 2H); 7,23–7.11 (m, 4H); 7.07 (dd, J = 7.5 Hz, 1.7 Hz, 2H); 7.06 (d, J = 560.6 Hz, 2H); 6.86 (dd, J = 8.1 Hz, 1.1 Hz, 2H); 6.75 (td, J = 7.4 Hz, 1.1 Hz, 2H); 6.13 (s, 1H) ppm. ^{31}P NMR (121.60 MHz/ 298 K/ [D$_6$]DMSO): δ = 17.13 ppm (s). TGA: T_{98} = 202 °C.

Crystal Data for $C_{24}H_{20}O_6P_2Zn$ (M = 531.71): orthorhombic, space group Iba2 (no. 45), a = 14.3215(6) Å, b = 18.7855(11) Å, c = 8.2191(3) Å, V = 2211.24(18) Å3, Z = 4, T = 150.15 K, $\mu(\text{Mo}K_\alpha)$ = 1.296 mm-1, $Dcalc$ = 1.597 g/mm³, 8231 reflections measured (4.34 ≤ 2Θ ≤ 52.12), 2143 unique (R_{int} = 0.0462, R$_{sigma}$ = 0.0298) which were used in all calculations. The final R_1 was 0.0312 (>2sigma(I)), and wR_2 was 0.0826 (all data).

2.2. Synthesis of Zinc(II)-bis(dibenzo[c,e][1,2]oxaphosphinin-6-olat-6-oxide) – $[Zn(DOPO\text{-}OH)_2]_n$

(A) Thermally induced oxidative ring closure of $[Zn(DOPO)_2]_n$

In a vacuum drying oven 5.32 g (10 mmol) of $[Zn(DOPO)_2]n$ were heated for 8 hours at 200 °C and 14 mbar. The product was obtained in quantitative yield.

Color: white; yield: 5.3 g, 100 %.

(B) Synthesis with DOPO-OH and zinc salt:

In a 400 mL beaker 22.32 g (100 mmol) of DOPO-OH were suspended in 100 mL of water. In a second beaker, 4.00 g (100 mmol) sodium hydroxide were dissolved. After cooling the solution to room temperature, the sodium hydroxide solution was dropped to the DOPO-OH suspension. The beaker was rinsed with water and a clear yellow solution was obtained. In a third beaker 6.81 g (50 mmol) zinc chloride were solved in 50 mL of water. The resulting solution was added to the other solution rapidly while stirring. The beaker was rinsed again with 25 mL of water, and a colorless solid appeared. The reaction mixture was stirred for 15 minutes. The

product was filtered, washed with water and dried in vacuo (5 mbar, 130 °C).

Color: White. Yield: 24.0 g, 90 %. ^{1}H NMR (299.90 MHz, 300 K, [D$_6$]DMSO): δ = 8.04 (ddd, J = 8.4 Hz, 5.1 Hz, 3.4 Hz, 4H); 7,90–7.78 (m, 2H); 7.63 (ddt, J = 8.3 Hz, 7.5 Hz, 1.2 Hz, 2H); 7,46–7.30 (m, 4H); 7,26–7.17 (m, 2H); 7.13 (dd, J = 8.0 Hz, 1.3 Hz, 2H) ppm. ^{31}P NMR (121.40 MHz/ 300 K/[D$_6$]DMSO): δ = 3.51 ppm (s). TGA: T$_{98}$ = 526 °C.

Crystal Data for C$_{24}$H$_{16}$O$_6$P$_2$Zn (M = 527.68): monoclinic, space group $P2_1/c$ (no. 14), a = 7.7641(4) Å, b = 24.5843(12) Å, c = 11.1920(7) Å, β = 99.545(4)°, V = 2106.7(2) Å3, Z = 4, T = 180.15 K, μ(MoK_α) = 1.360 mm-1, Dcalc = 1.664 g/mm3, 15808 reflections measured (4.96 ≤ 2Θ ≤ 52.42), 4145 unique (R_{int} = 0.0735, R$_{sigma}$ = 0.0699) which were used in all calculations. The final R_1 was 0.0354 (>2sigma(I)) and wR_2 was 0.0749 (all data).

2.3. Synthesis of Poly(auqua-bis((2'-hydroxy-[1,1'-biphenyl]-2-yl)phosphinato)Calcium(II)) – [Ca(DOPO)$_2$(H$_2$O)]$_n$

The synthesis of [Ca(DOPO)$_2$(H$_2$O)]$_n$ was performed in the same way like [Zn(DOPO)$_2$]$_n$. 108.09 g (500 mmol) DOPO, 20.00 (500 mmol) sodium hydroxide and 37.76 g (250 mmol) calcium chloride dihydrate were used. The colorless solid appeared after 30 min. stirring. After a reaction time of 14 hours, the solid was filtered, washed with water and dried in vacuo (8 mbar, 50 °C).

Color: white; yield: 122.1 g, 93 %. ^{1}H NMR (299.90 MHz, 297 K, [D$_6$]DMSO): δ = 10.11 (bs, 2H); 7.98 (t, J = 9.8 Hz, 2H); 7,46–7.34 (m, 2H); 7,33–7.23 (m, 2H); 7.17 (td, J = 7.0 Hz, 2.1 Hz, 4H); 7,13–7.05 (m, 2H); 7.05 (d, 519.7 Hz, 2H); 6.92 (dd, J = 8.4 Hz, 1.2 Hz, 2H); 6.84 (td, J = 7.4 Hz, 1.2 Hz, 2H); 3.39 (s, 2H) ppm. ^{31}P NMR (121.40 MHz/ 298 K/[D$_6$]DMSO): δ = 6.32 ppm (bs). TGA: T$_{98}$ = 153 °C.

Crystal Data for C$_{24}$H$_{22}$O$_7$P$_2$Ca (M = 524.43): monoclinic, space group P2$_1$ (no. 4), a = 11.9210(10) Å, b = 7.8082(4) Å, c = 13.1695(11) Å, V = 1164.42(16) Å3, Z = 2, T = 180 K, μ(MoK_α) = 0.451 mm-1, Dcalc = 1.496 g/mm^3, 7287 reflections measured (4.34 ≤ 2Θ ≤ 52.12), 3989 unique (R_{int} = 0.0657, R$_{sigma}$ = 0.0406) which were used in all calculations. The final R_1 was 0.0542 (>2sigma(I)) and wR_2 was 0.0897 (all data).

2.4. Synthesis of Calcium-bis(dibenzo[c,e][1,2]oxaphosphinin-6-olat-6-oxide) – [Ca(DOPO-OH)$_2$]$_n$

In a 200 mL beaker, 5.00 g (21.5 mmol) of DOPO-OH were dissolved in 50 mL of methanol. The mixture was stirred and 0.86 g (21.5 mmol) sodium hydroxide was added. In a second beaker, 1.39 (10.8 mmol) calcium chloride dihydrate were dissolved in 50 mL of methanol. While stirring vigorously, the calcium chloride salt solution was added rapidly to the clear DOPO-OH solution. A colorless solid was obtained. The reaction mixture was stirred for 15 minutes. The product was filtered, washed with water and dried in vacuo (3 mbar, 100 °C).

Color: White. Yield: 5.3 g, 97 %. ^{1}H NMR (299.90 MHz, 297 K, [D$_6$]DMSO): δ = 8,63–6.76 (m, 16H). ^{31}P NMR (121.40 MHz/ 297 K/[D$_6$]DMSO): δ = –0.37 ppm (bs); –1.75 ppm (bs). TGA: T$_{98}$ = 519 °C.

2.5. Synthesis of Poly(bis((2'-hydroxy-[1,1'-biphenyl]-2-yl)phosphinato)magnesium(II)) [Mg(DOPO)$_2$]

In a 100 mL beaker 8.43 g (38.9 mmol) of DOPO were suspended in 40 mL of water. 1.56 g (38.9 mmol) sodium hydroxide in 20 mL of water was dropped into the solution of DOPO in water. A clear solution was obtained. In a second beaker 4.99 g (19.49 mmol) magnesium nitrate hexahydrate were solved in 20 mL of water. The salt solution was added to the other solution rapidly while stirring. The beaker was rinsed with 10 mL of methanol. The reaction mixture was stirred overnight, and the solvent was removed by filtra-

tion. The product was washed with water and dried in vacuo (5 mbar, 50 °C).

Color: white; yield: 4.68 g, 48.96 %. ^{1}H NMR (300.38 MHz, 298 K, [D$_6$]DMSO): δ = 10.18 (bs, 2H); 7.90–7.87 (m, 2H); 7.44–7.39 (td, J = 7.50 Hz, 7.47 Hz, 1.45 Hz, 2H); 7.34–7.29 (m,2H); 7.21–7.06 (m, 8H); 6.89–6.81 (dd, J = 15.86 Hz, 7.69 Hz, 4H); ^{31}P NMR (121.60 MHz/ 298 K/[D$_6$]DMSO): δ = 9.84 ppm (s). TGA: T$_{98}$ = 174 °C.

2.6. Synthesis of [Mg(DOPO-OH)$_2$(H$_2$O)$_6$]

In a 100 mL beaker 9.06 g (41.89 mmol) of DOPO-OH was suspended in 40 mL of water. 1.56 g (41.89 mmol) sodium hydroxide in 20 mL of water was dropped into the solution of DOPO in water. A clear solution was obtained. In a second beaker 5.37 g (20.94 mmol) magnesium nitrate hexahydrate were solved in 20 mL of water. The salt solution was added to the other solution rapidly while stirring. The beaker was rinsed with 10 mL of water. The reaction mixture was stirred overnight, and the solvent was removed by filtration. The product was washed with water and dried in vacuo (5 mbar, 130 °C).

Color: white; yield: 5.14 g, 51.24 %. ^{1}H NMR (300.38 MHz, 298 K, [D$_6$]DMSO): δ = 8.21–7.11 (m, 16H); ^{31}P NMR (121.60 MHz/ 298 K/ [D$_6$]DMSO): δ = –1.84 ppm (s). TGA: T$_{98}$ = 370 °C.

Crystal Data for C$_{24}$H$_{32}$MgO$_{14}$P$_2$ (M = 630.74 g/mol): monoclinic, space group C2/$_c$ (no. 15), a = 35.017(3) Å, b = 6.8644(5) Å, c = 11.9573(11) Å, β = 93.978(7)°, V = 2867.3(4) Å^3, Z = 4, T = 180.15 K, μ(MoK_α) = 0.242 mm-1, Dcalc = 1.461 g/cm^3, 10445 reflections measured (4.664° ≤ 2Θ ≤ 50.498°), 2583 unique (R_{int} = 0.1784, R$_{sigma}$ = 0.1243) which were used in all calculations. The final R_1 was 0.0754 [$I > 2\sigma(I)$] and wR_2 was 0.1938 (all data).

2.7. Synthesis of Poly(bis((2'-hydroxy-[1,1'-biphenyl]-2-yl)phosphinato)bis(N-methylimidazole)zinc(II)) [Zn(DOPO)$_2$(NMI)$_2$]

In a 100 mL beaker, 7.27 g (33.6 mmol) of DOPO were dissolved in 75 mL of methanol. 5.52 g (5.4 mL; 67.0 mmol) N-Methylimidazole was dropped into the solution of DOPO in methanol. A clear solution was obtained. In a second beaker, 5.00 g (19.50 mmol) zinc nitrate hexahydrate were solved in 75 mL of methanol. The salt solution was added to the other solution rapidly while stirring. The beaker was rinsed with 10 mL of methanol. The reaction mixture was stirred overnight and the solvent was removed by filtration. The product was washed with water and dried in vacuo (5 mbar, 60 °C).

Color: white; yield: 10.5 g, 95 %. ^{1}H NMR (300.38 MHz, 298 K, [D$_6$]DMSO): δ = 7.74–7.71 (m, 1H); 7.55–7.49 (m, 1H); 7.47 (m, 1H); 7.40–7.35 (m, 2H); 7.30 (m, 1H); 7.20–7.15 (m, 3H); 7.08–7.05 (m, 1H); 6.89–6.86 (m, 1H); 6.80–6.74 (m, 1H); 3.78 (s, 3H); ^{31}P NMR (121.60 MHz/ 298 K/[D$_6$]DMSO): δ = 16.63 ppm (s). TGA: T$_{98}$ = 152 °C.

Crystal Data for C$_{32}$H$_{32}$N$_4$O$_6$P$_2$Zn (M = 695.92 g/mol): triclinic, space group P$\bar{1}$ (no. 2), a = 7.5080(2) Å, b = 15.3850(4) Å, c = 28.6062(8) Å, α = 105.541(2)°, β = 94.292(2)°, γ = 90.020(2)°, V = 3173.86(15) Å^3, Z = 4, T = 180.15 K, μ(MoK_α) = 0.925 mm^{-1}, Dcalc = 1.456 g/cm^3, 53747 reflections measured (4.448° ≤ 2Θ ≤ 51.4°), 11934 unique (R_{int} = 0.0614, R$_{sigma}$ = 0.0532) which were used in all calculations. The final R_1 was 0.0345 [$I > 2\sigma(I)$] and wR_2 was 0.0778 (all data).

Acknowledgments

[1] a) B. Xing, M. F. Choi, B. Xu, *Chem. Eur. J.* **2002**, *8*, 5028–5032; b) S. J. Shearan, N. Stock, F. Emmerling, J. Demel, P. A. Wright, K. D. Demadis, M. Vassaki, F. Constantino, R. Vivani, S. Sallard, *Crystals* **2019**, *9*, 270.

[2] O. Oms, J. Le Bideau, A. Vioux, D. Leclercq, *J. Organomet. Chem.* **2005**, *690*, 363–370.

[3] a) C. Pettinari, F. Marchetti, N. Mosca, G. Tosi, A. Drozdov, *Polym. Int.* **2017**, *66*, 731–744; b) Y. Hou, W. Hu, Z. Gui, Y. Hu, *Ind. Eng. Chem. Res.* **2017**, *56*, 2036–2045; c) B. Burk, Ruprechts-Karl-Universität Heidelberg **2016**; d) M. D. Ahlmann, U. D. Dittrich, M. P. D. Döring, B. D. Just, H. D. Keller, U. D. Storzer, **2006**.

[4] a) G. P. Funkhouser, N. Tonmukayakul, F. Liang, *Langmuir* **2009**, *25*, 8672–8677; b) B. P. Block, G. H. Dahl, L. R. Ocone, N. D. Peschko, US3522178A, **1970**; c) W. D. C. D. Racky, H. J. D. C. D. Kleiner, W. D. C. D. Herwig, **1974**; d) M.-J. Zhou, B. Li, L. Liu, Y.-L. Feng, J.-Z. Guo, *CrystEngComm* **2014**, *16*, 10034–10039.

[5] B. P. Block, S. H. Rose, C. W. Schaumann, E. S. Roth, J. Simkin, *J. Am. Chem. Soc.* **1962**, *84*, 3200–3201.

[6] a) E. Oleshkevich, C. Viñas, I. Romero, D. Choquesillo-Lazarte, M. Haukka, F. Teixidor, *Inorg. Chem.* **2017**, *56*, 5502–5505; b) B. Moulton, M. J. Zaworotko, *Curr. Opin. Solid State Mater. Sci.* **2002**, *6*, 117–123.

[7] a) S.-J. Liu, R. J. Staples, J. P. Fackler Jr., *Polyhedron* **1992**, *11*, 2427–2430; b) S. H. Rose, B. P. Block, *J. Am. Chem. Soc.* **1965**, *87*, 2076–2077; c) B. P. Block, J. Simkin, *Inorg. Chem.* **1963**, *2*, 688–690; d) S. H. Rose, B. P. Block, *J. Polym. Sci., Part A-1:. Polym. Chem.* **1966**, *4*, 573–582.

[8] G. M. Kosolapoff, J. S. Powell, *J. Chem. Soc. (Resumed)* **1950**, 3535–3538.

[9] S. R. Sandler, US4180495A, **1979**.

[10] S. D. Hörold, W. D. Wanzke, DE102007037019A1, **2009**.

[11] K. Xanthopoulos, Z. Anagnostou, S. Chalkiadakis, D. Choquesillo-Lazarte, G. Mezei, J. K. Zaręba, J. Zoń, K. D. Demadis, *Crystals* **2019**, *9*, 301.

[12] E. Oleshkevich, I. Romero, F. Teixidor, C. Viñas, *Dalton Trans.* **2018**, *47*, 14785–14798.

[13] a) K. A. Salmeia, S. Gaan, *Polym. Degrad. Stab.* **2015**, *113*, 119–134; b) M. Rakotomalala, S. Wagner, M. Döring, *Materials* **2010**, *3*, 4300–4327.

[14] Y. S. A. Nakajima, JP 63284243, **1988**.

[15] S. T. I. K. H. Hisashi, JP2001139586A, **2001**.

[16] W. Wehner, WO2014060004A1, **2014**.

[17] M. D. Ahlmann, U. D. Dittrich, M. P. D. Döring, B. D. Just, H. D. Keller, U. D. Storzer, DE102004049614A1, **2006**.

[18] A. K. Katz, J. P. Glusker, S. A. Beebe, C. W. Bock, *J. Am. Chem. Soc.* **1996**, *118*, 5752–5763.

[19] a) W. Rothwell, *J. Am. Chem. Soc.* **1993**, *105*, 2637–2640; b) P. Gerbier, C. Guérin, B. Henner, J.-R. Unal, *J. Mater. Chem.* **1999**, *9*, 2559–2565.

[20] R. K. Brow, C. C. Phifer, G. L. Turner, R. J. Kirkpatrick, *J. Am. Ceram. Soc.* **1991**, *74*, 1287–1290.

[21] R. D. Shannon, *Acta Crystallogr., Sect. A* **1976**, *32*, 751–767.

[22] M. Leistner, R. Pfaendner, D. Trupti, H. G. Köstler, W. Wehner, DE102013210902A1, **2014**.

[23] G. METz, X. Wu, S. O. Smith, *J. Magn. Reson., Ser. A* **1994**, *110*, 219–227.

[24] A. E. Bennett, C. M. Rienstra, M. Auger, K. Lakshmi, R. G. Griffin, *J. Chem. Phys.* **1995**, *103*, 6951–6958.

[25] O. V. Dolomanov, L. J. Bourhis, R. J. Gildea, J. A. Howard, H. Puschmann, *J. Appl. Crystallogr.* **2009**, *42*, 339–341.

[26] G. M. Sheldrick, *Acta Crystallogr., Sect. A: Foundations. Crystallogr.* **2008**, *64*, 112–122.

[27] G. M. Sheldrick, *Acta Crystallogr., Sect. C: Struct. Chem.* **2015**, *71*, 3–8.

[28] W.-L. Lee, L.-C. Liu, C.-M. Chen, J.-S. Lin, *Polym. Adv. Technol.* **2014**, *25*, 36–40.